

Nanoscale

Accepted Manuscript



This is an *Accepted Manuscript*, which has been through the Royal Society of Chemistry peer review process and has been accepted for publication.

Accepted Manuscripts are published online shortly after acceptance, before technical editing, formatting and proof reading. Using this free service, authors can make their results available to the community, in citable form, before we publish the edited article. We will replace this *Accepted Manuscript* with the edited and formatted *Advance Article* as soon as it is available.

You can find more information about *Accepted Manuscripts* in the [Information for Authors](#).

Please note that technical editing may introduce minor changes to the text and/or graphics, which may alter content. The journal's standard [Terms & Conditions](#) and the [Ethical guidelines](#) still apply. In no event shall the Royal Society of Chemistry be held responsible for any errors or omissions in this *Accepted Manuscript* or any consequences arising from the use of any information it contains.

Cite this: DOI: 10.1039/c0xx00000x

www.rsc.org/xxxxxx

ARTICLE TYPE

High Quality Liquid-type Quantum Dots White Light-Emitting Diode

Chin-Wei Sher,^a Chin-Hao Lin,^b Huang-Yu Lin,^b Chien-Chung Lin,^{*c} Che- Hsuan Huang,^b Kuo-Ju Cher^b
Jie-Ru Li,^b Kuan-Yu Wang,^c Hsien-Hao Tu,^b Chien-Chung Fu,^a and Hao-Chung Kuo,^{*b,d}

Received (in XXX, XXX) Xth XXXXXXXXX 20XX, Accepted Xth XXXXXXXXX 20XX

DOI: 10.1039/b000000x

This study demonstrates a novel package design to store colloidal quantum dots in liquid format and integrate it with standard LED. The high efficiency and high quality color performance for neutral white correlated color temperature can be demonstrated. The experimental results indicate that the liquid-type quantum dots white light-emitting diode (LQD WLED) is highly efficient and reliable. The luminous efficiency and color rendering index (CRI) of the LQD WLED can reach to $271 \text{ lmW}_{\text{op}}^{-1}$ and 95 respectively. Moreover, the glass box is employed to prevent from humidity and oxygen erosion. With this encapsulation design, our quantum dot box can survive over 1000 hours of on-self storage time.

Introduction

Recently, colloidal quantum dots (QDs) have attracted industrial attention because of their unique properties such as high quantum yield, minimal backscattering, size dependent tunable bandgap, and narrow emission full width at half maximum.¹⁻⁷ As a novel technology in this field, QDs offer more varieties in color mixing. In the past, high quantum efficiency and an excellent color-rendering index were achieved by multishell QDs and co-doping QDs in phosphor.^{3,8} Core-shell structures have been employed to enhance the quantum yield of QDs and derive high photoluminescence efficiency.^{8,9} QD can also be applied in some premium products such as displays with high color gamut and WLEDs.¹⁰⁻¹⁴ As for the methods to dispense QDs, several groups have reported successful results in transfer printing¹², pulsed spray¹, inkjet printing¹¹ and mist coating¹⁴. Furthermore, the 30 nm emission bandwidth of the QDs can yield a higher degree of color purity compared with the estimated 100 nm bandwidth of the monochromatic phosphor-converted LEDs.^{15,16}

One major concern in these QD devices is the reduction in quantum efficiency when the solvent is dried up. When the QDs are dispensed in solvent, their light emission capability is much better than in the solid phase, due to the self-aggregation effect¹⁷. Another issue accompanying with solidification is the so-called "coffee ring" effect which results from the migration of the solutes toward the edge of the droplets during drying process.¹⁹

In this study, liquid-type QD White LED is demonstrated as an efficient color-conversion layer in UV LED packages. We use glass material to protect quantum dots material from drying. This method can increase quantum dots efficiency and reliability. The white liquid-type quantum dots LED can be demonstrated with high color rendering index (CRI) at 4360K of correlated color temperature (CCT).

Experiment

In the sample preparation, two types of devices were fabricated at the same time for comparison: one is the remote QD type (as our reference sample), and the other is the liquid type QD device. Fig. 1(a) show the structure and process flow of remote structure QD. We use PDMS to fill the 5070 type package. After PDMS material is cured, an illuminating layer which contains QD and PMMA was dispensed on the LED package surface. To pump these QDs, a UV LED chip was installed in this 5070 package. The UV LED chips are first attached to the sub-mount. Then, the gold-wire bonding method was used to connect the anode and cathode pads. The chip size is 45mil x 45mil and the nominal power output of the UV chip (SemiLEDs EV-D45A) is 240 mW at 350 mA and the emission wavelength is 365 nm at 350 mA driving current. The real device measurement yields the UV optical power (watts) electrical power (watt)⁻¹ ratio is 0.091 or 9.1%. Fig. 1 (b) illustrates the process flow of liquid-type QD White LED. The procedure is as follows: First, the glass substrate was cut into thin stripes with the size of 3.0 cm x 1.5 cm. Second, take four of these thin stripes and sandwich them in between two larger pieces of glass. Third, proper gap was left such that the air can ventilate when liquid QDs was injected. Finally, the gap were sealed with epoxy-based glue to finish the liquid QD process. The thickness of the glass slide is 0.1cm and thus the overall volume which can accommodate QD solution is $1.5\text{cm} \times 3\text{cm} \times 0.1\text{cm} = 0.45 \text{ cm}^3 = 0.45 \text{ ml}$. The silicone is applied into 5070 cup by direct dispensing method. Under normal operation, the UV LED is based at 100mA and the normal power is 43mW. Considering the area of 5070 package, which is 0.25 cm^2 , the pumping intensity is 172.8 mWcm^{-2} . Both remote quantum dots structure and liquid-type quantum dots structure were fabricated with same quantum dots and characterized under the same conditions (i.e. same UV chip initial brightness, and same humidity and temperature).

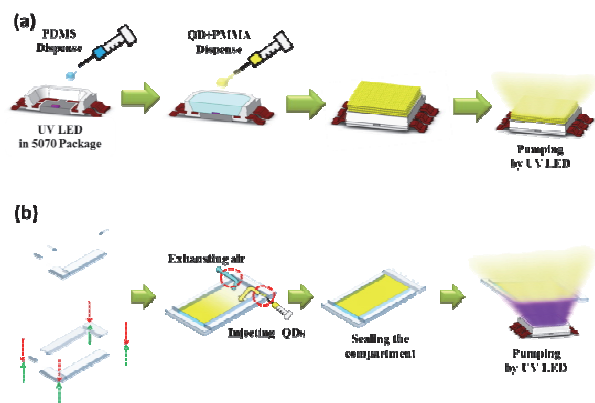


Fig. 1. (a)(b). Process flow of remote structure QD white LED and liquid-type QD white LED.

As for QD characterization, we use Horiba, FL-3 system to measure the spectrum and intensity. Fig. 2(a) (b) shows the UV-visible absorption and photoluminescence (PL) spectra of five QD species used in this experiment. Our QDs were purchased from UT Dots, Inc. (web site: <http://www.utdots.com>). The QDs are dissolved in xylenes and different sizes of the dots can provide different emission wavelengths. To have emission wavelength of each QD sitting within $\pm 10\text{nm}$ of the specification, certain control on the dot size distribution is necessary. The full width of half maximum (FWHM) of the emission spectrum is normally less than 35nm for all products. The surface stabilizers of the dots are either octadecylamine (green and red) or oleic acid (blue and blue-green) and the concentration is 5mg mL^{-1} . The photoluminescence quantum yield (PLQY) of all QDs is higher than 50% according to vendor's datasheet. From the experimental result, the wavelengths of blue, blue-green, green, orange, and red components were located at 450nm, 490nm, 535nm, 590nm and 630nm, respectively. The FWHM of these emission spectra are approximately 20, 40, 40, 35, and 40 nm, respectively. Fig. 2 (c) and Fig. 2 (d) show the completed liquid type QD glass without and with UV pumping. The surrounding environment is totally dark when we took the picture of Fig. 2(d). So instead of white light, the strong scattering of the residual blue photons from the UV lamp (model number: UVGL-58) masked the weaker visible ones from QDs and the whole film would look like blue.

When the QDs with different colors were mixed, optimized procedures were carried out to obtain similar CCTs and best CRI values. The quantity of each color of QD can determine the final color quality of the device. Microbalances were used to precisely measure the weight of each type of QD. The weight percentages for the reference and liquid QD samples were listed in Table. 1.

Table 1. The QD weight percentages for each type of sample.

wavelength (nm)	450	490	535	590	630
Liquid QD	53.33%	13.34%	13.34%	13.34%	6.66%
Remote QD	57.70%	11.34%	11.34%	13.80%	5.82%

Measurement and analysis

Figures 3(a) and (b) show the EL spectra of the remote QD type and liquid QD type devices under the injection currents from 20mA to 250 mA. The inset in Fig. 3(a) is the current-dependent integrated intensity extracted from Fig. 3(a) and (b). All the

measurements were performed in a calibrated integrated sphere. From the data, we see an overall improvement of 66.6 % between liquid and remote samples at 250 mA driving current. To analyze in more details, the incremental percentages of the blue, blue-green, green, orange, and red color bands are 14.6%, 37.8%, 38.9%, 29.4%, and 39.4%, respectively at 250mA driving current.

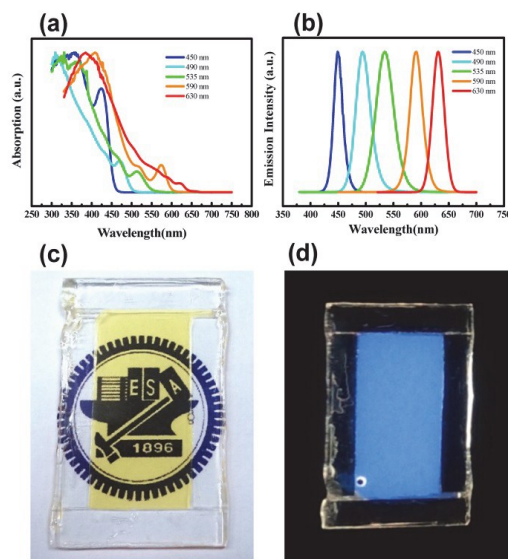


Fig. 2. (a) Absorption spectra and (b) emission spectra of blue, blue-green, green, orange, and red QDs. (c) liquid-type QD in the glass package before UV LED pumping (d) liquid-type QD in the glass package pumping by uniform UV light.

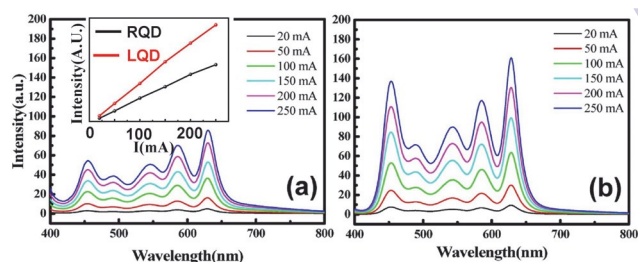


Fig. 3. (a) conventional remote QD and (b) liquid-type QD emission spectra of blue, blue-green, green, orange, and red QDs. The inset in (a) is the current-dependent integrated intensity of two types of devices.

The luminous efficacy of radiation (LER) is one of the indicators to show how efficient the emitter is in terms of white light generation. To calculate LER, one can use the following expression²⁰:

$$LER = 683 \frac{\text{lm}}{\text{W}} \frac{\int V(\lambda) P_{\text{white}}(\lambda) d\lambda}{\int P_{\text{white}}(\lambda) d\lambda} \quad (1)$$

where 683 lm W^{-1} is a normalization factor, $V(\lambda)$ is the human eye sensitivity function, and $P_{\text{white}}(\lambda)$ is the spectral power density of the light source. In Fig. 4 (a), the LER of the LED device with liquid-type quantum dots is approximately $271 \text{ lm W}_{\text{op}}^{-1}$, and this value is higher than $78 \text{ lm W}_{\text{op}}^{-1}$ of the remote quantum dots structure. This improvement can be attributed to high quantum yield of the liquid type device. In addition, Fig. 4(b) demonstrates the current-dependent CRI of both devices. In average, the CRI values are very stable and exceed 90 in different current levels. This characteristic is brought by the five colors of QDs in the spectra which can fulfill the CRI requirement.

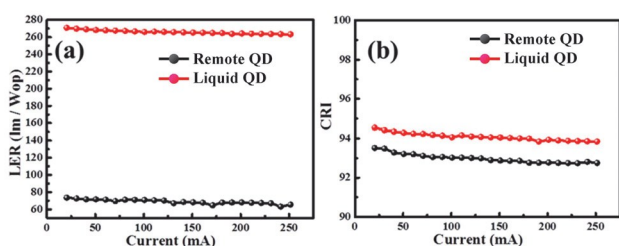


Fig. 4. Current-dependent (a) luminous efficacy of radiation (LER) of UV LED with conventional remote QDs and liquid QDs (b) color rendering index (CRI) of UV LED with conventional remote QD and liquid-type QDs.

To verify the claim that liquid type device can preserve the quantum yield, one key factor to be tested is the PLQY of the QD LED. Because the QD layer is optically pumped by a UV source, the efficiency to convert the UV photons into visible ones can be expressed as^{21,22}

$$PLQY = \frac{\int_{\text{visible_band}} \left(\frac{\lambda}{hc} \right) \times [I_{em}^{QD}(\lambda) - I_{em}^{ref}(\lambda)] d\lambda}{\int_{UV_band} \left(\frac{\lambda}{hc} \right) \times [I_{ex}^{ref}(\lambda) - I_{ex}^{QD}(\lambda)] d\lambda} \quad (2)$$

where I_{ex}^{QD} and I_{ex}^{ref} are the integrated intensities of the UV excitation with and without the QD layer, and I_{em}^{QD} and I_{em}^{ref} are the spectral intensities of the visible band with and without the QD layer, respectively. By using the spectra of samples with and without QD layer, we can estimate the PLQY values for both types of devices. The PLQY of the liquid QD device is 33.87% and the reference remote QD sample is 31.32%. The number for liquid QD case can be re-adjusted to 34% if the UV absorption of the glass slides, which is about 10% usually, is taken into account. A higher PLQY value of liquid type device also justify our initial idea on keeping QDs from solidification.

Figure 5(a)-(c) shows that the thermal images at the surfaces of a regular LED, remote quantum dots and liquid-type quantum dots samples. Fig. 5(d) shows the current dependent surface temperatures among these three different types of devices. The surface temperature can reach 200°C at 250mA in the remote case. This will reduce the efficiency of quantum dots and cause reliability problem²³. On the other hand, the liquid type QD LED can keep the surface temperature as low as 50°C, which is advantageous towards both performance and reliability. As for the temporal behavior of the sample under UV excitation, surface thermal image measurements on the similar setup which contains QDs wrapped in silicone like material with UV LED packaged together was performed. The stabilization of the surface temperatures both under high and low current injection is within 5 minutes based on the 30-minute observation.

To investigate the huge difference in the surface temperatures, we must understand more on the thermal transport characteristics of the package materials. The thermal conductivity of the glass is $1.05 \text{ W (m}\cdot\text{K)}^{-1}$ and PMMA is $0.167\text{-}0.25 \text{ W (m}\cdot\text{K)}^{-1}$. Apparently the glass container of the liquid type device is a much better material for heat dissipation and the glass slides also possess much larger area. Invoking the Fourier's law of heat conduction, we could obtain the thermal resistance (R) calculated as²⁴:

$$\text{heat - transfer - rate} = \frac{\Delta T}{R}; R \propto \frac{L}{\kappa A} \quad (3)$$

where ΔT is the temperature difference between two endpoints and R is the thermal resistance. In this simplified model, we could observe the significant difference made by the thermal conductivity and area of the device. From the calculation of effective emission area, the heat dissipation capacity between Remote QD and Liquid QD can be very different. The effective area of liquid QD sample is 1.34cm^2 and the other device is only 0.25 cm^2 . Combining with the different material, a much larger thermal resistance (33.7 times under one-dimensional analysis) in the remote QD case is expected. That is the major cause for much higher surface temperature detected. High heat trapped inside the package can certainly reduce the efficiency of QDs while the liquid QD will have larger footprint and take up more space for setup.

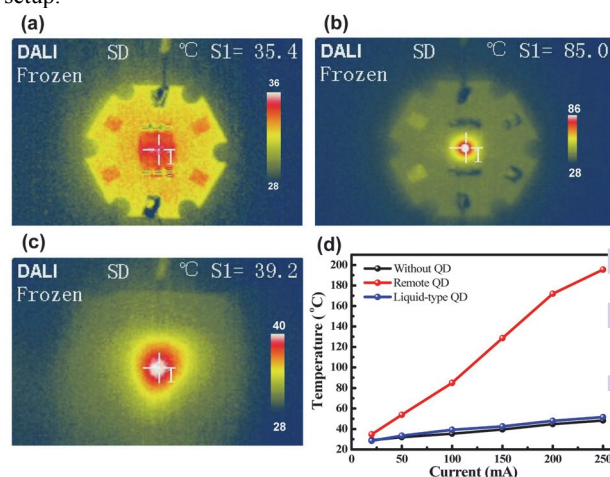


Fig. 5. The IR images of surface temperature in (a) without quantum dots, (b) remote quantum dots white LED and (c) liquid-type quantum dot white LED at driving current = 100 mA. Fig.5 (d) show the temperature and current's relation of two different quantum dots structure.

The Fig. 6 (a)-(b) shows the white light images of the remote quantum dots structure and liquid-type quantum dots structure under UV LED excitation. The pictures of Figs. 6(a) and (b) were taken by the generic digital camera (HTC[®] One[®]) and imported into Matlab[®] to extract the two-dimensional intensity profile in Fig. 6(c). By properly choosing the ratio between different QDs, both devices can achieve similar CCT (4500K) and high CRI (>90). The effective emission areas for liquid QD and reference QD samples are quite different. From the 2D intensity profile as shown in the Fig. 6(c), the emission area of the liquid QD device can be estimated as 1.34cm^2 , which is about five times of the reference. But at the same time, due to the controlled output power of UV LEDs, the excitation source is kept the same; thus the comparison between the two types of samples should solely depend on the emission efficiency of quantum dots. Large emission area can be helpful for thermal dissipation (as can be observed in the Fig. 5) and further maintain the quantum yield of the QD solution in our case, which eventually contributes to better LER. The uniformity of the light intensity, if defined by the 10% variation of the maximum, can be as high as 91.2% of the emission area. Meanwhile, the luminous efficiency of the liquid QD device is about $7 \text{ lumen watt (electrical power)}^{-1}$.

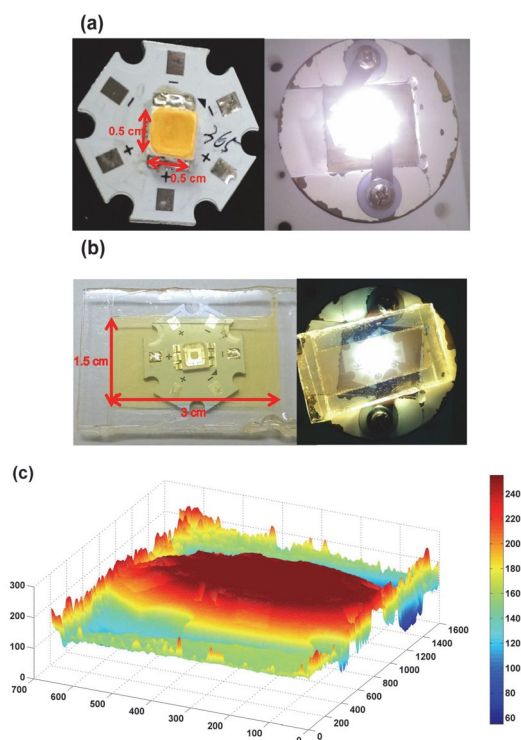


Fig. 6. Image of the (a) remote quantum dots structure under UV excitation, (b) liquid-type quantum dots structure under UV excitation. (c) The 2D intensity profile of the liquid QD in (b).

After initial characterization of the devices, the next important task is to test the longevity of this liquid QD LED. In the past, many results have shown serious degradation of the QD performance when the device is exposed to air^{7, 17, 25}. In our design, the glass container was sealed to prevent the solvent from drying and also keep oxygen and water from reacting with QDs. We hope this can help to preserve the quantum yield of the QDs over a long period of time. Figures 7(a) and (b) show the emission spectra of a remote QD structure and liquid-type QDs structure taken at various time as we store both devices in the room temperature. The measurement condition for both devices is at 350mA driving current and the measurements were tested at 0, 0.15, 0.3, 0.4, 0.5, 1, 20, 40, 72, 350, 500 and 1000 hours. The experimental result demonstrates that the liquid-type quantum dots structure has stable and sustainable performance over a long period of time, as shown in Fig. 7 (c). The efficiency reductions of the remote quantum dots structure and liquid-type quantum dots structure are 75% and 5% after 1000 hours of storage respectively. The color rendering index shifts of the remote quantum dots structure and liquid-type quantum dots structure at 350mA current from 0 to 1000 hours are shown in Fig. 7(d). It is found that the color rendering indices of both structures quickly become stable after 0.5 hours. From these results, the liquid type of package not only maintains its intensity but also its color quality over a long storage time.

One concern about possible change of QD size distribution rises when the QD is stored in liquid phase. With current test condition, which does not constantly shine the QD samples with UV photons, the interference from UV heating could be minimized. On the other hand, the self-aggregation of QDs in liquid phase for

a long storage time should be discussed. To evaluate this without performing TEM, the emission spectrum of the QD layer holds the key. The emission spectrum of a QD ensemble usually represents the size distribution of this ensemble²⁶, because the size of nanoparticle can determine the emission peak wavelength and the population of the same sized particle is proportional to the emission intensity. So the direct comparison between the peak positions and FWHM of emission spectra can help us to understand the size distribution of the dots and thus the degree of aggregation. Fig. 7(b) provides a great opportunity for evaluating each QD's variation during this long storage time. By using proper curve fitting, the position and FWHM of each peak can be found and the results are summarized in Table 2.

From this table, we could observe very little changes between 0th and 1000th hour of testing among the five different QDs we put into the glass slide. Certainly the nature of this storage test minimized the extreme thermal and UV illumination issues for the sample, but the constant performance and minimum aggregation that can be implicated from this table demonstrate a potential solution for the long-term stability in this QD type of devices.

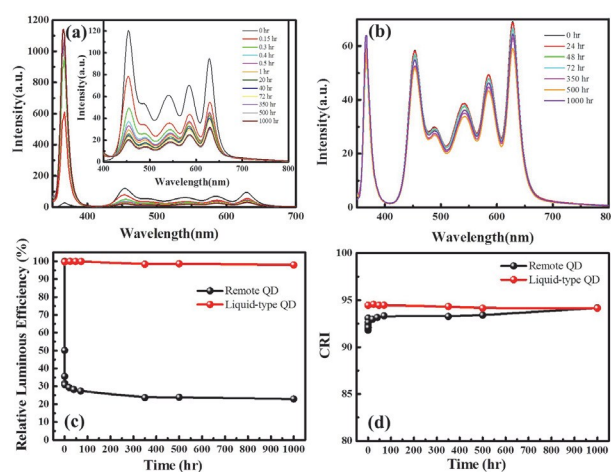


Fig. 7. (a) The relative emission spectrum of the remote quantum dots white light LED structure with various life times (0, 0.15, 0.3, 0.4, 0.5, 1, 20, 40, 72, 350, 500 and 1000 hours, from top to bottom curves) (b) The relative emission spectrum of the liquid-type quantum dots white light LED structure with various life times (0, 24, 48, 72, 350, 500 and 1000 hours, from top to bottom curves). The life time character of (c) changing about relative luminous efficiency and (d) CRI between remote quantum dots and liquid-type quantum dots structure white LED from 0 hours to 1000 hours.

Table 2. The comparison of the linewidths and peaks among different QDs and elapsed time.

Parameters	Elapsed Time	QD1	QD2	QD3	QD4	QD5
Linewidth (nm)	0th hour	22.67	45.94	44.67	26.84	24.35
	1000th hour	23.51	46.99	43.88	26.84	25.21
Peak (nm)	0th hour	451.93	484.72	541.27	585.10	627.21
	1000th hour	451.46	485.36	542.25	585.13	627.40

For the quantum dots white LED, the color deviation with the different structure is used to evaluate the color stability for high-

quality lighting applications. Therefore, the chromaticity coordinate shifts of remote quantum dots and liquid-type quantum dots structure are recorded and shown in Figs. 8(a) and (b). As the time passed by, the chromaticity coordinates for liquid-type quantum dots structure are stable. Moreover, the color deviation of a lighting system, ($\Delta u'v'$) is calculated as follows²⁷:

$$u' = 4x/(-2x+12y+3) \quad (4)$$

$$v' = 9y/(-2x+12y+3) \quad (5)$$

$$\Delta u'v' = \sqrt{(\Delta u')^2 + (\Delta v')^2} \quad (6)$$

, where u' , v' is the chromaticity coordinates in the CIE 1976 diagram, and x and y are the chromaticity coordinates in the CIE 1931 diagram. The $\Delta u'v'$ value indicates color shifts which might alter the CCT eventually. From the experimental results, remote QD sample showed moderate CIE coordinate-shift while the liquid QD sample kept almost the same after 1000 hours of storage time. This clearly demonstrates the superiority of our design in terms of light quality which should be crucial for the next generation source.

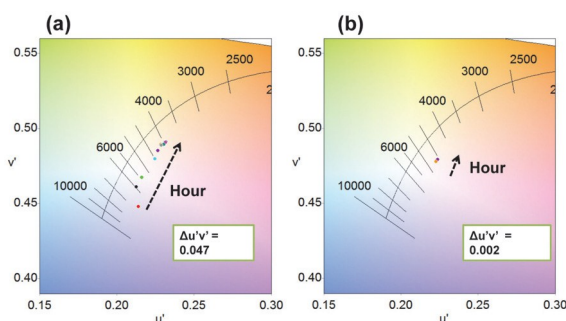


Fig. 8. (a) The color shift character of remote quantum dots structure white LED from 0 hours to 1000 hours. (b) The color shift character of liquid-type quantum dots structure white LED from 0 hours to 1000 hours.

Conclusion

This study demonstrates a hybrid white LED with the liquid-type quantum dots structure to produce a stable and high color rendering index light source. We use a glass-slide-formed cavity to protect quantum dots from environmental influences. Liquid-type quantum dot structure can maintain quantum dot efficiency and reduce the thermal effect. This design can modify the emission spectrum easily and enhance the quantum yield of QDs. The finished WLED, when pumped by UV LED in the package, can achieve a LER of $271 \text{ lm W}_{\text{op}}^{-1}$ and 5% decrease after 1000 hours of storage. We believe that the liquid-type quantum dots WLED with high lumen efficiency is suitable for various high quality lighting applications in the near future.

Funding Sources

This work was funded by the National Science Council in Taiwan under grant numbers MOST 101-2221-E-009-046-MY3, MOST104-3113-E-009-002-CC2, MOST102-2221-E-009-131-MY3, and MOST103-2622-E-009-008-CC3.

Notes and references

- ^a Department of Power Mechanical Engineering, National Tsing Hua University, Taiwan R.O.C, No. 101, Section 2, Kuang-Fu Road, Hsinchu 30013, Taiwan; Email: steven.sher@hotmail.com
- ^b Department of Photonics & Institute of Electro-Optical Engineering, National Chiao Tung University, Hsinchu 30010, Taiwan; Email: hckuo@faculty.nctu.edu.tw
- ^c Institute of Photonic System, National Chiao Tung University, Tainan 711, Taiwan. Fax: +886-6-3032535; Tel: +886-6-3032121#57754; Email: chienchunglin@faculty.nctu.edu.tw
- ^d Department of Electrical Engineering, Da Yeh University, Changhua 51591, Taiwan
1. K.-J. Chen, H.-C. Chen, K.-A. Tsai, C.-C. Lin, H.-H. Tsai, S.-H. Chien, B.-S. Cheng, Y.-J. Hsu, M.-H. Shih, C.-H. Tsai, H.-H. Shi and H.-C. Kuo, *Advanced Functional Materials*, 2012, **22**, 5138-5143.
 2. P. Gu, Y. Zhang, Y. Feng, T. Zhang, H. Chu, T. Cui, Y. Wang, J. Zhao and W. W. Yu, *Nanoscale*, 2013, **5**, 10481-10486.
 3. H. S. Jang, H. Yang, S. W. Kim, J. Y. Han, S.-G. Lee and D. Y. Jeor, *Advanced Materials*, 2008, **20**, 2696-2702.
 4. J. Lee, V. C. Sundar, J. R. Heine, M. G. Bawendi and K. F. Jensen, *Advanced Materials*, 2000, **12**, 1102-1105.
 5. I. L. Medintz, H. T. Uyeda, E. R. Goldman and H. Mattoussi, *Mater*, 2005, **4**, 435-446.
 6. P. Reiss, J. Bleuse and A. Pron, *Nano Lett.*, 2002, **2**, 781-784.
 7. Y. Shirasaki, G. J. Supran, M. G. Bawendi and V. Bulovic, *Nat Photon*, 2013, **7**, 13-23.
 8. E. Jang, S. Jun, H. Jang, J. Lim, B. Kim and Y. Kim, *Advanced Materials*, 2010, **22**, 3076-3080.
 9. F. Ren, H. Zhao, F. Vetrone and D. Ma, *Nanoscale*, 2013, **5**, 7800-7804.
 10. C. Dang, J. Lee, Y. Zhang, J. Han, C. Breen, J. S. Steckel, S. Coe-Sullivan and A. Nurmikko, *Advanced Materials*, 2012, **24**, 5915-5918.
 11. H. M. Haverinen, R. A. Myllylä and G. E. Jabbour, *Applied Physics Letters*, 2009, **94**, 073108.
 12. T.-H. Kim, K.-S. Cho, E. K. Lee, S. J. Lee, J. Chae, J. W. Kim, D. H. Kim, J.-Y. Kwon, G. Amaratunga, S. Y. Lee, B. L. Choi, Y. Kuk, J. M. Kim and K. Kim, *Nat Photon*, 2011, **5**, 176-182.
 13. Y.-C. Pu and Y.-J. Hsu, *Nanoscale*, 2014, **6**, 3881-3888.
 14. T. Zhu, K. Shanmugasundaram, S. C. Price, J. Ruzyllo, F. Zhang, J. Xu, S. E. Mohny, Q. Zhang and A. Y. Wang, *Applied Physics Letters*, 2008, **92**, 023111.
 15. J. H. Oh, J. R. Oh, H. K. Park, Y.-G. Sung and Y. R. Do, *Opt Express*, 2012, **20**, A1-A12.
 16. J. R. Oh, S.-H. Cho, H. K. Park, J. H. Oh, Y.-H. Lee and Y. Rag, *Opt Express*, 2010, **18**, 11063-11072.
 17. K.-S. Cho, E. K. Lee, W.-J. Joo, E. Jang, T.-H. Kim, S. J. Lee, S.-J. Kwon, J. Y. Han, B.-K. Kim, B. L. Choi and J. M. Kim, *Nat Photon*, 2009, **3**, 341-345.
 18. S. Nizamoglu, T. Ozel, E. Sari and H. V. Demir, *Nanotechnology*, 2007, **18**, 065709.
 19. A. Kshirsagar, S. Pickering, J. Xu and J. Ruzyllo, *ECS Transactions*, 2011, **35**, 71-77.
 20. T. Erdem, S. Nizamoglu and H. V. Demir, *Opt Express*, 2012, **20**, 3275-3295.
 21. K. Suzuki, A. Kobayashi, S. Kaneko, K. Takehira, T. Yoshihara, H. Ishida, Y. Shiina, S. Oishi and S. Tobita, *PCCP*, 2009, **11**, 9850-986

-
22. S.-C. Hsu, Y.-H. Chen, Z.-Y. Tu, H.-V. Han, S.-L. Lin, T.-M. Chen, H.-C. Kuo and C.-C. Lin, 2015.
23. K.-J. Chen, H.-C. Chen, M.-H. Shih, C.-H. Wang, M.-Y. Kuo, Y.-C. Yang, C.-C. Lin and H.-C. Kuo, *Journal of Lightwave Technology*, 2012, **30**, 2256-2261.
- 5 24. F. Incropera and D. DeWitt, "Introduction to Heat Transfer", Fourth Edition, John Wiley & Sons, Inc., 2002.
25. J. Kwak, W. K. Bae, D. Lee, I. Park, J. Lim, M. Park, H. Cho, H. Woo, D. Y. Yoon, K. Char, S. Lee and C. Lee, *Nano Lett.*, 2012, **12**, 2362-2366.
- 10 26. S. Crooker, J. Hollingsworth, S. Tretiak and V. Klimov, *Phys. Rev. Lett.*, 2002, **89**, 186802.
27. H.-T. Huang, C.-C. Tsai and Y.-P. Huang, *Opt. Express*, 2010, **18**, A201-A206.
- 15